Supplementary Material

Comparative assessment of the ELBA coarse-grained model for water

Mario Orsi

School of Engineering & Materials Science, Queen Mary University of London
Mile End Road, London E1 4NS, United Kingdom

m.orsi@qmul.ac.uk
www.orsi.sems.qmul.ac.uk

Shifted-force interactions

The total potential energy U_{ij} of an interacting pair of ELBA water sites i, j is:

$$U_{ij} = U_{ij}^{\mathrm{LJ}} + U_{ij}^{\mathrm{dip}},$$

with U_{ij}^{LJ} the Lennard-Jones term and U_{ij}^{dip} the point dipole term.

Shifted-force Lennard-Jones interaction The shifted-force form of the Lennard-Jones potential is [1]:

$$U_{ij}^{\mathrm{LJ}} = 4\epsilon \left\{ \left[\left(\frac{\sigma}{r}\right)^{12} - \left(\frac{\sigma}{r}\right)^{6} \right] + \left[6\left(\frac{\sigma}{r_c}\right)^{12} - 3\left(\frac{\sigma}{r_c}\right)^{6} \right] \left(\frac{r}{r_c}\right)^{2} - 7\left(\frac{\sigma}{r_c}\right)^{12} + 4\left(\frac{\sigma}{r_c}\right)^{6} \right\},$$

where r is the interparticle distance, r_c is the cutoff radius, and σ and ϵ have the standard meaning [2]. The corresponding force is given by:

$$\boldsymbol{f}_{ij} = \left\{ \left[48\epsilon \left(\frac{\sigma}{r}\right)^{12} - 24\epsilon \left(\frac{\sigma}{r}\right)^{6} \right] \frac{1}{r^2} - \left[48\epsilon \left(\frac{\sigma}{r_c}\right)^{12} - 24\epsilon \left(\frac{\sigma}{r_c}\right)^{6} \right] \frac{1}{r_c^2} \right\} \boldsymbol{r}$$

where $\boldsymbol{r}$ is the pair distance vector, $\boldsymbol{r} = \boldsymbol{r}_i - \boldsymbol{r}_j$.

Shifted-force point dipole interaction Considering two point dipoles $\boldsymbol{\mu}_i$ and $\boldsymbol{\mu}_j$, the shifted-force pair potential energy is:

$$U_{ij}^{\mathrm{dip}} = \left[1 - 4\left(\frac{r}{r_c}\right)^{3} + 3\left(\frac{r}{r_c}\right)^{4} \right] \left[\frac{1}{r^3}(\boldsymbol{\mu}_i \cdot \boldsymbol{\mu}_j) - \frac{3}{r^5}(\boldsymbol{\mu}_i \cdot \boldsymbol{r})(\boldsymbol{\mu}_j \cdot \boldsymbol{r}) \right]$$

where $\boldsymbol{r}$ and r are the pair distance vector and its magnitude, respectively, and r_c is the cutoff distance. The standard factor $(4\pi\varepsilon_0)^{-1}$ is assumed, and omitted for clarity here and in the following formulae. Note that we use the convention $\boldsymbol{r} = \boldsymbol{r}_i - \boldsymbol{r}_j$. Forces and torques were derived following the approach in Appendix C.3 of Allen and Tildesley [2]. In particular, the pair forces are:

$$\begin{aligned} \boldsymbol{f}_{ij} = -\boldsymbol{f}_{ji} \quad = \quad & \frac{3}{r^5} \left\{ \left[1 - \left(\frac{r}{r_c}\right)^{4} \right] \left[(\boldsymbol{\mu}_i \cdot \boldsymbol{\mu}_j) - \frac{3}{r^2}(\boldsymbol{\mu}_i \cdot \boldsymbol{r})(\boldsymbol{\mu}_j \cdot \boldsymbol{r}) \right] \boldsymbol{r} + \right. \\ & \left. \left[1 - 4\left(\frac{r}{r_c}\right)^{3} + 3\left(\frac{r}{r_c}\right)^{4} \right] \left[(\boldsymbol{\mu}_j \cdot \boldsymbol{r})\boldsymbol{\mu}_i + (\boldsymbol{\mu}_i \cdot \boldsymbol{r})\boldsymbol{\mu}_j - \frac{2}{r^2}(\boldsymbol{\mu}_i \cdot \boldsymbol{r})(\boldsymbol{\mu}_j \cdot \boldsymbol{r})\boldsymbol{r} \right] \right\} \end{aligned}$$

The pair torque $\boldsymbol{\tau}_{ij}$ is:

$$\boldsymbol{\tau}_{ij} = -\frac{1}{r^3} \left[1 - 4\left(\frac{r}{r_c}\right)^{3} + 3\left(\frac{r}{r_c}\right)^{4} \right] (\boldsymbol{\mu}_i \times \boldsymbol{\mu}_j) + \frac{3}{r^5} \left[1 - 4\left(\frac{r}{r_c}\right)^{3} + 3\left(\frac{r}{r_c}\right)^{4} \right] (\boldsymbol{\mu}_j \cdot \boldsymbol{r})(\boldsymbol{\mu}_i \times \boldsymbol{r})$$

The pair torque $\boldsymbol{\tau}_{ji}$ is:

$$\boldsymbol{\tau}_{ji} = -\frac{1}{r^3} \left[1 - 4\left(\frac{r}{r_c}\right)^{3} + 3\left(\frac{r}{r_c}\right)^{4} \right] (\boldsymbol{\mu}_j \times \boldsymbol{\mu}_i) + \frac{3}{r^5} \left[1 - 4\left(\frac{r}{r_c}\right)^{3} + 3\left(\frac{r}{r_c}\right)^{4} \right] (\boldsymbol{\mu}_i \cdot \boldsymbol{r})(\boldsymbol{\mu}_j \times \boldsymbol{r})$$

The expressions above, for both the Lenard-Jones and the point dipole potential, have been implemented in the `pair_lj_sf_dipole_sf.cpp` module of the program LAMMPS [3].

Integration timestep and energy conservation

Compared to previous publications [4, 5], in this work we have reduced the inertial features of the ELBA water model. In particular, we have here set a realistic mass of $18\,\mathrm{g\,mol^{-1}}$, and a principal moment of inertia of $30\,\mathrm{g\,Å^2\,mol^{-1}}$. In the original model [4], values of respectively $40\,\mathrm{g\,mol^{-1}}$ and $100\,\mathrm{g\,Å^2\,mol^{-1}}$ were chosen to permit a stable integration of the equations of motion with a 15 fs timestep; this choice was made to maximise the efficiency of serial simulations, as at the time the in-house software used did not allow parallel calculations. Since the ELBA model is now available in the parallel program LAMMPS [3], maximising the timestep is less critical, and we have decided to reduce the timestep size to permit the setting of a realistic (lower) mass.

The timestep choice was validated by running NVE simulations and monitoring the total energy. In particular, Figure S1 reports the time evolution of the total energy for a range of timesteps from 5 to 15 fs.

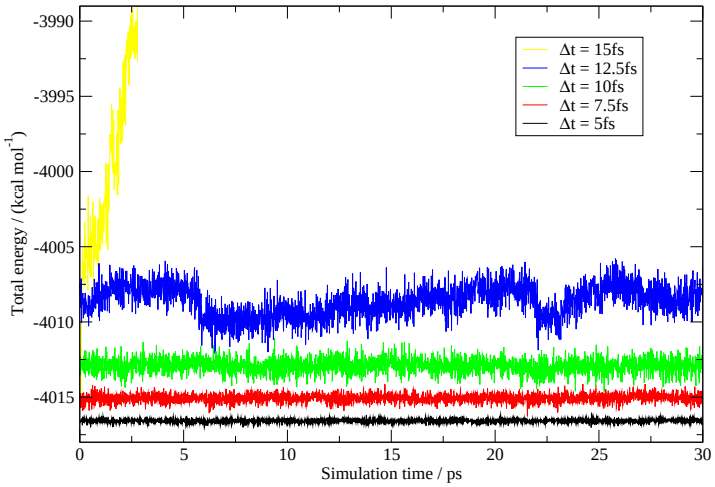

Figure S1: Total energy conservation for different integration timesteps. For clarity, the different data sets were shifted up or down to avoid overlaps.

It can be seen that the total energy is conserved accurately up to $\Delta t = 10$ fs. A larger timestep of 12.5 fs could still be acceptable; over 30 ps, while the energy oscillates slightly (within 0.1%), there is no net drift. For $\Delta t = 15$ fs, the total energy is clearly not conserved.

The fluctuations in potential, kinetic, and total energy as a function of the Δt are displayed in Figure S2.

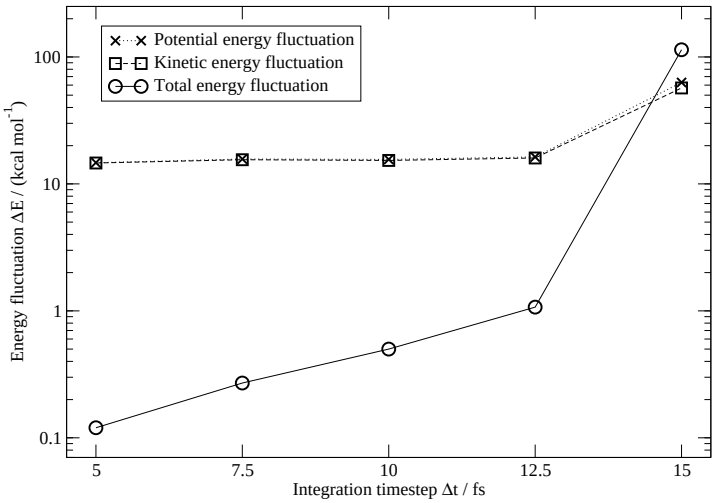

Figure S2: Average energy fluctuation $\Delta E = \sqrt{\langle (E - \langle E \rangle)^2 \rangle}$.

For timesteps up to 12.5 fs, the average fluctuation in the total energy is at least 10 times smaller than the average fluctuations in both the potential and kinetic energy, satisfying recommended criteria [6].

Overall, our choice of $\Delta t = 10\,\mathrm{fs}$ for production simulations should guarantee accurate and robust integration of the equations of motion.

Computational timings

Simulations of a liquid-vapour interface comprising 8000 water molecules were run for the single-site ELBA coarse-grained model, a representative 3-site model (SPC), and a representative 4-site model (TIP4P/2005). For each model, the same parameters reported in the main body of the paper were used; in particular, the timestep was 10 fs for ELBA and 2 fs for the atomistic models, and the cutoff radii were 1.2, 1.0 and 1.3 nm for respectively ELBA, SPC and TIP4P/2005. The calculations were run on a GNU/Linux cluster of 2.66 GHz Intel "Westmere" processors based on 2 sockets and 12 processors per node, with QLogic TrueScale interconnect. Figure S3 reports a comparison in terms of *sampling speed*, defined as *number of ns sampled / day*, where *day* is intended in terms of calculation (wall-clock) time.

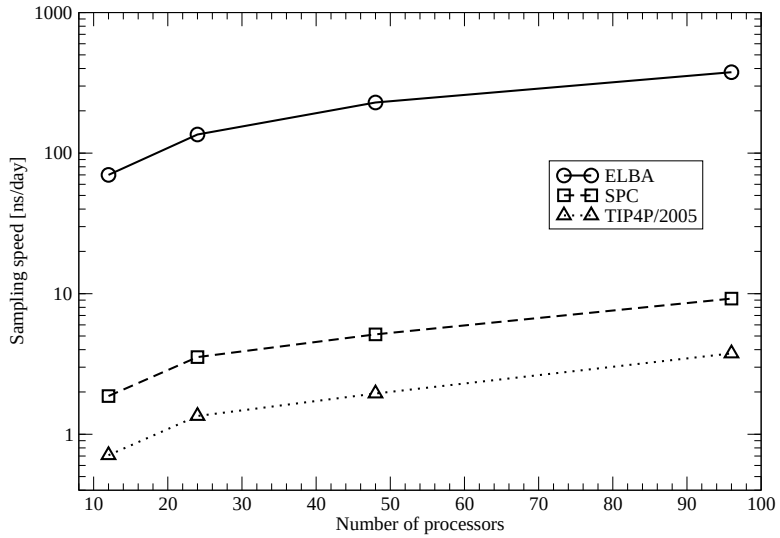

Figure S3: Comparison of sampling speed between representative water models. Simulations were run on 12, 24, 48 and 96 processors. Note the logarithmic scale used to represent the sampling speed.

It can be seen that the speed up factors in the ELBA simulations are respectively ≈ 40 and ≈ 100 compared to SPC and TIP4P/2005. It is also clear that such factors are rather insensitive to the number of processors employed.

Mean square displacement and time-dependent diffusion curves

The mean square displacement (MSD) was obtained with:

$$MSD = \frac{1}{N}\sum_{i=1}^{N}[\mathbf{r}_i(t) - \mathbf{r}_i(0)]^2 \tag{1}$$

with N the number of water molecules, t the time, and $\mathbf{r}_i$ the 3-dimensional vector defining the position of particle i. Figure S4 shows the MSD from the liquid bulk simulations of each model. The self-diffusion coefficient D was obtained from the bulk systems using the standard expression [7]:

$$D = \frac{MSD}{6t} \tag{2}$$

where MSD is defined in Eq. 1 and t is the simulation time; see Fig. S5.

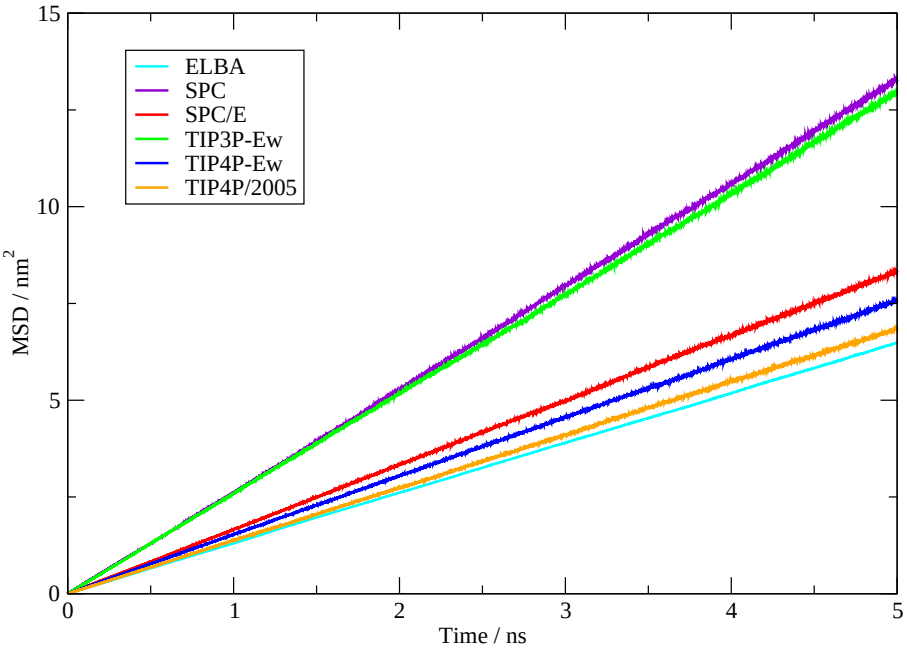

Figure S4: Mean square displacement as a function of simulation time.

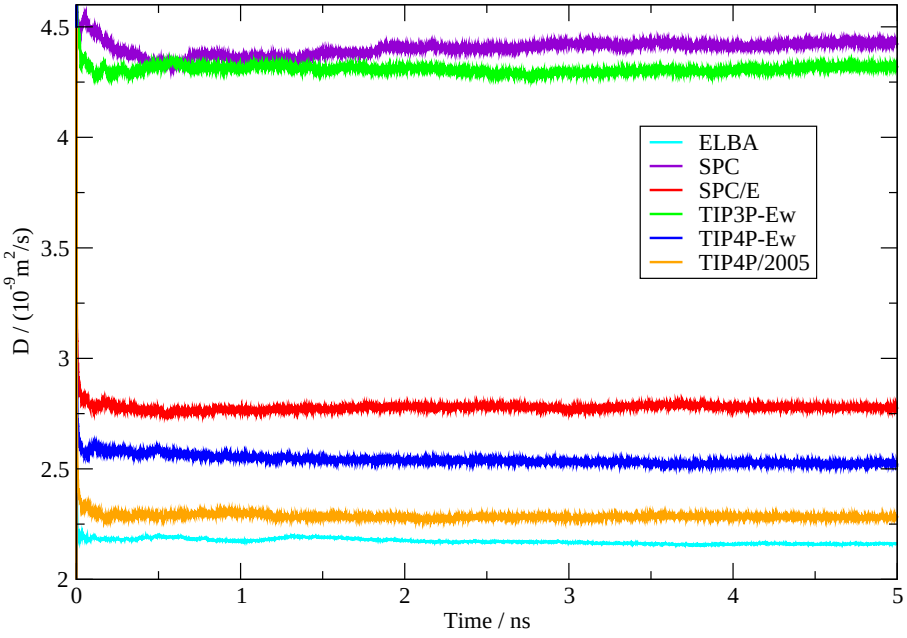

Figure S5: Self-diffusion coefficient as a function of simulation time.

Radial distribution function: main peaks

	$g_{OO}(r_1)$	r_1/Å	$g_{OO}(r_2)$	r_2/Å
SPC	2.85	2.77	1.06	4.56
SPC/E	3.08	2.74	1.11	4.50
TIP3P-Ew	2.91	2.70	1.07	4.41
TIP4P-Ew	3.18	2.76	1.14	4.43
TIP4P/2005	3.23	2.77	1.14	4.44
ELBA	2.66	3.10	1.22	5.97
Experiment [8]	2.75	2.73	1.16	4.50

Table S1: Properties of the radial distribution function for bulk water at 298 K and 1 atm. Height of first peak: $g_{OO}(r_1)$. Location of first peak: r_1. Height of second peak: $g_{OO}(r_2)$. Location of second peak: r_2. Relative uncertainties are $< 0.1\%$.

Mass density profiles

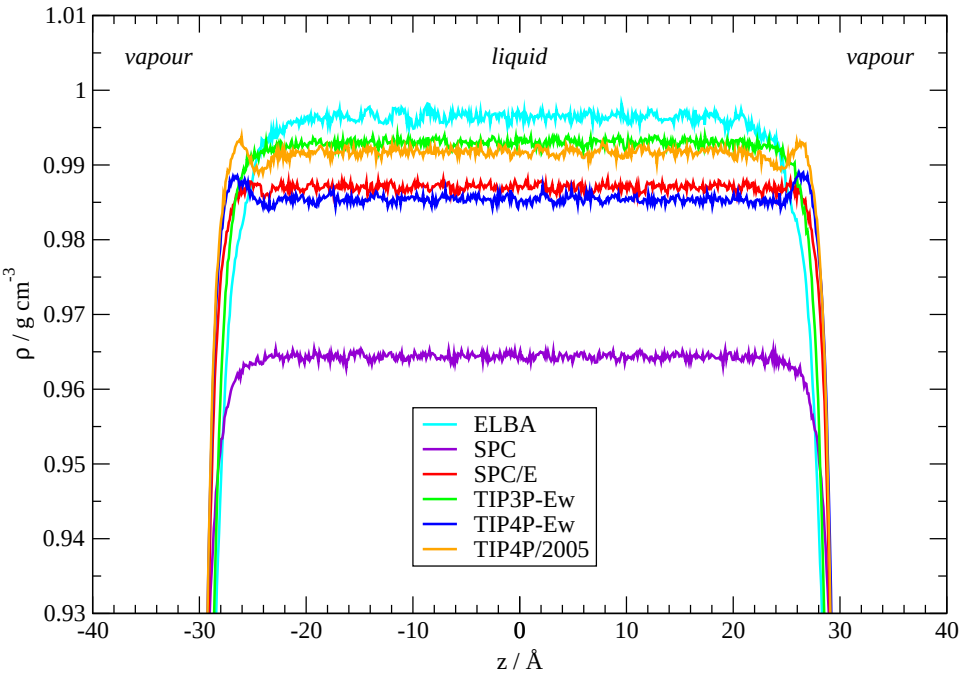

Figure S6: Mass density profiles. It can be noticed that the TIP4P-like models feature small yet non-negligible density peaks at the liquid-vapour interfaces. In previous work, such peaks were observed to disappear with increasing system size [9].

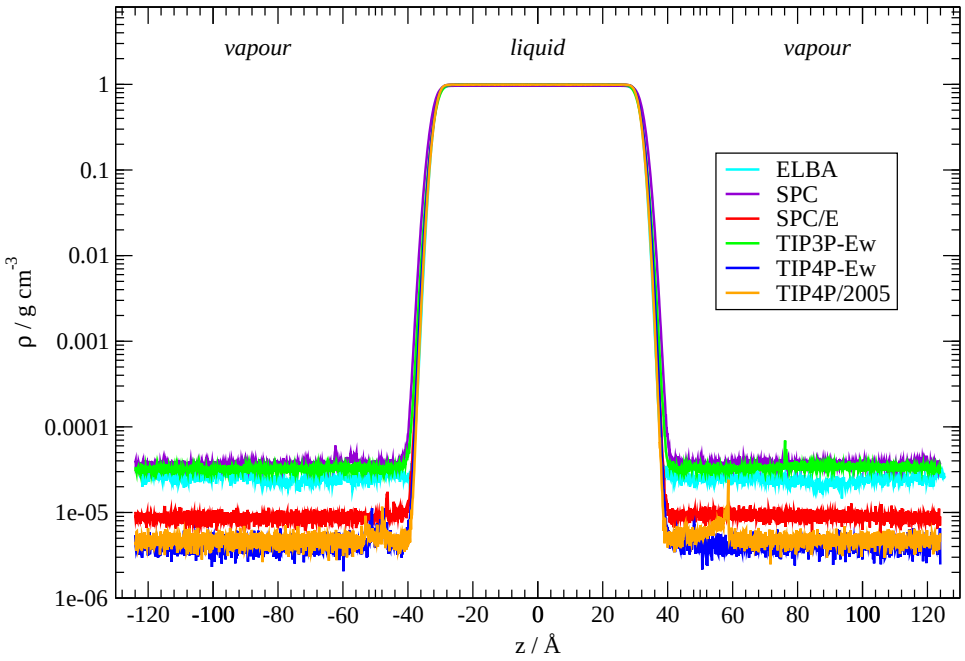

Figure S7: Mass density profiles. To facilitate interpretation in the vapour regions, the density is displayed using a logarithmic scale. For the liquid region, see Figure S6.

Electrostatic potential and electric field profiles

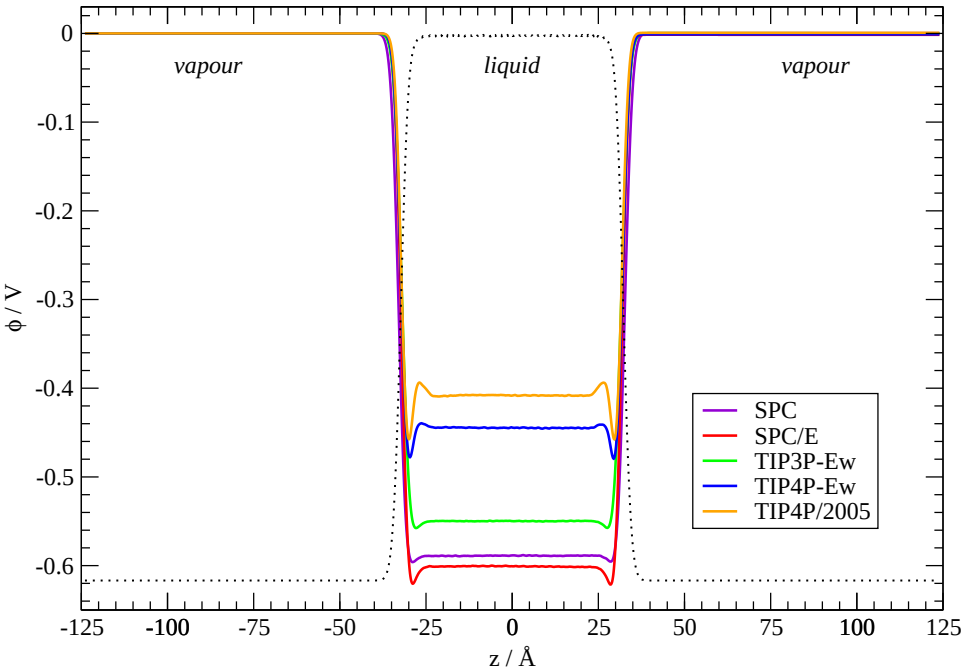

Figure S8: Electrostatic potential profiles. For convenience, a representative mass density profile is also shown with a dotted line (ordinate values not on scale).

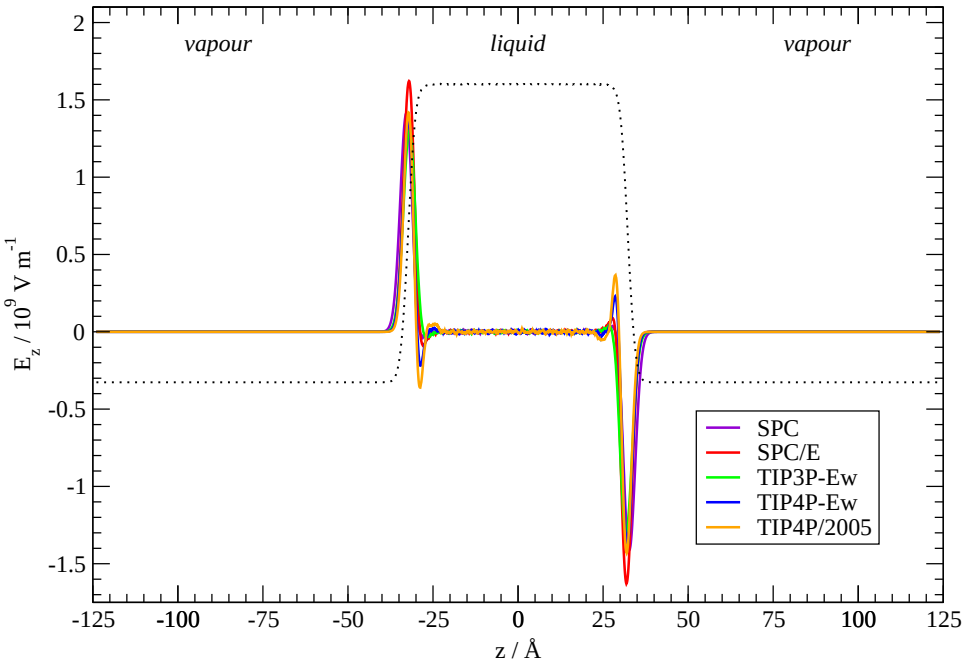

Figure S9: Electric field profiles. For convenience, a representative mass density profile is also shown with a dotted line (ordinate values not on scale).

References

[1] S.D. Stoddard and J. Ford, Phys. Rev. A **8**, 1504 (1973).

[2] M.P. Allen and D.J. Tildesley, *Computer Simulation of Liquids*, 1st ed. (Oxford Science Publications, Oxford, 1987).

[3] S. Plimpton, J. Comp. Phys. **117**, 1 (1995), `http://lammps.sandia.gov`.

[4] M. Orsi and J.W. Essex, PLoS ONE **6**, e28637 (2011).

[5] M. Orsi and J.W. Essex, Faraday Discuss. **161**, 249 (2013).

[6] S. Riniker and W.F. van Gunsteren, J. Chem. Phys. **134**, 084110 (2011).

[7] D.C. Rapaport, *The Art of Molecular Dynamics Simulation*, 2nd ed. (Cambridge University Press, Cambridge, 2004).

[8] A. Soper, Chem. Phys. **258**, 121 (2000), `www.isis.stfc.ac.uk`.

[9] J. Alejandre and G.A. Chapela, J. Chem. Phys. **132**, 014701 (2010).